

Sharp Feature in the Pseudogap of Quasicrystals Detected by NMR

X.-P. Tang,¹ E. A. Hill,¹ S. K. Wonnell,¹ S. J. Poon,² and Y. Wu¹

¹Department of Physics and Astronomy, University of North Carolina, Chapel Hill, North Carolina 27599-3255

²Department of Physics, University of Virginia, Charlottesville, Virginia 22901

(Received 13 January 1997)

The ²⁷Al and ⁶³Cu spin-lattice relaxation rates were found to contain a large T^2 term over a wide temperature range below 400 K in several thermodynamically stable quasicrystalline alloys, including *i*-AlCuRu, *i*-AlPdRe, *i*-AlCuFe, and the crystalline approximant phase α -AlMnSi. The relaxation mechanism is proven to be electronic in origin. Such nonlinear temperature dependence is shown to be a clear signature of sharp features in the density of states at the Fermi level. The estimated width of this sharp feature is on the order of 20 meV. [S0031-9007(97)03655-7]

PACS numbers: 61.44.Br, 71.20.-b, 76.60.-k

Quasicrystals possess novel structures with long-range order and point group symmetry incompatible with periodicity [1]. Structurally ordered quasicrystalline metallic alloys also exhibit novel transport properties, including very high electrical resistivity and semi-insulating behavior [2,3]. A pseudogap of about 0.5–1.0 eV in width at the Fermi level E_F was shown both experimentally [4–8] and theoretically [9] to be a generic property of quasicrystals and approximants. Such a pseudogap could contribute significantly to the thermodynamic stability of quasicrystals, but it is too broad to account for the novel transport properties [9]. Band structure calculations show that spiked peaks and valleys of density of states (DOS) with widths of 10–50 meV are present in the broad pseudogap, and such sharp features could be related to the novel transport properties [9]. High resolution photoemission spectroscopy (PES) reveals a broad pseudogap in several quasicrystalline alloys; however, no sharp DOS features are observed [6,7]. Since PES only probes the near surface layers, sharp features in the pseudogap could be removed by subtle structural deviations near the surface from that of the bulk. Subtle structural deviations near the surface have been observed by scanning tunneling microscopy studies of annealed quasicrystal surfaces [10]. However, tunneling spectroscopy studies of quasicrystals have provided evidence of a sharp DOS valley at E_F with a width of about 50 meV [8] even though this technique is also sensitive to surface structures. In contrast to PES and tunneling spectroscopy, magnetic susceptibility [11] and nuclear magnetic resonance (NMR) [12] studies probe bulk properties; signatures of sharp DOS features at E_F could be revealed by these techniques. In this work, novel NMR results in the quasicrystalline and approximant phases are presented and explained, demonstrating unambiguously the presence of a sharp DOS valley at the Fermi level.

Icosahedral quasicrystals $Al_{65}Cu_{20}Ru_{15}$ (*i*-AlCuRu), $Al_{62.5}Cu_{24.5}Fe_{13}$ (*i*-AlCuFe), $Al_{70}Pd_{20}Re_{10}$ (*i*-AlPdRe), and the crystalline approximant $Al_{72.5}Mn_{17.4}Si_{10.1}$ (α -AlMnSi) were investigated. For comparison, two crystalline nonapproximants, the metallic ω phase Al_7Cu_2Fe (ω -AlCuFe) and the semiconducting Al_2Ru , were also studied.

Samples were vacuum sealed in quartz tubes for NMR experiments. The ²⁷Al, ⁶³Cu, and ⁶⁵Cu NMR measurements were performed selectively on the central transition at 9.4 T. The signal was detected by the Hahn echo technique, and the nuclear spin-lattice relaxation rates were obtained by the inversion recovery method [12].

Figure 1(a) shows ²⁷Al spectra of *i*-AlPdRe at 9.4 T which are characteristic of Al-based quasicrystals and approximants. The shifts in the quasicrystals and the approximant are very small with respect to the aqueous $Al(NO_3)_3$ solution and are noticeably temperature dependent, as illustrated in Fig. 1(a).

If the spin lattice relaxation is dominated by hyperfine couplings between nuclear and electron spins, the inversion

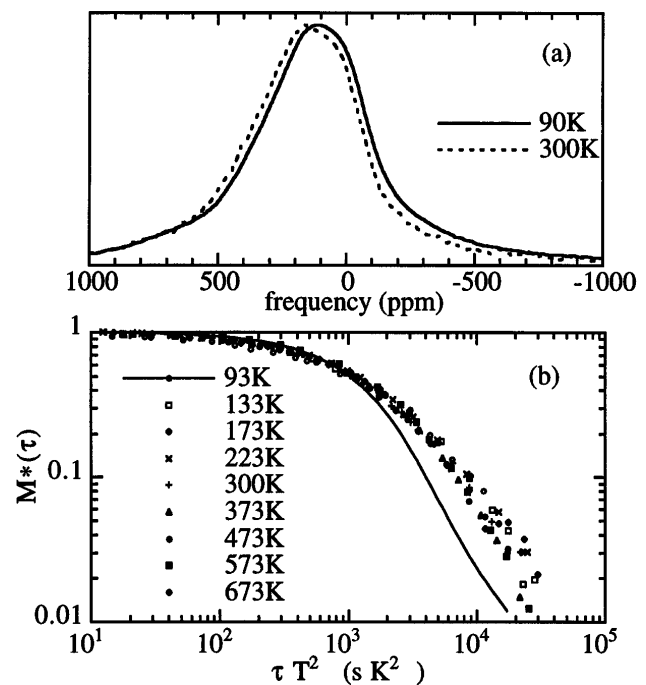


FIG. 1. (a) the ²⁷Al spectra of *i*-AlPdRe. (b) The inversion recovery curves of magnetization M versus τ which is scaled by T^2 at the corresponding temperature in *i*-AlPdRe and $M^* \equiv [M(\infty) - M(\tau)]/[M(\infty) - M(0)]$.

recovery of the magnetization $M(\tau)$ associated with the central transition for spin- $\frac{5}{2}$ nuclei is governed by

$$M(\tau) = M_\infty [1 - 0.057 \exp(-2W_1\tau) - 0.356 \exp(-12W_1\tau) - 1.587 \exp(-30W_1\tau)], \quad (1)$$

where τ is the recovery time after the magnetization inversion. The spin-lattice relaxation rate is defined as $1/T_1 \equiv 2W_1$. Figure 2 shows the temperature dependence of $1/T_1$ obtained by a least-squares fit of the inversion-recovery curve with Eq. (1). The fits, as shown in Fig. 1(b), deviate from the measured curves at long τ as observed before [13,14]. However, the temperature dependence of $1/T_1$ can also be confirmed by scaling τ for each temperature, as demonstrated in Fig. 1(b); this procedure is independent of the func-

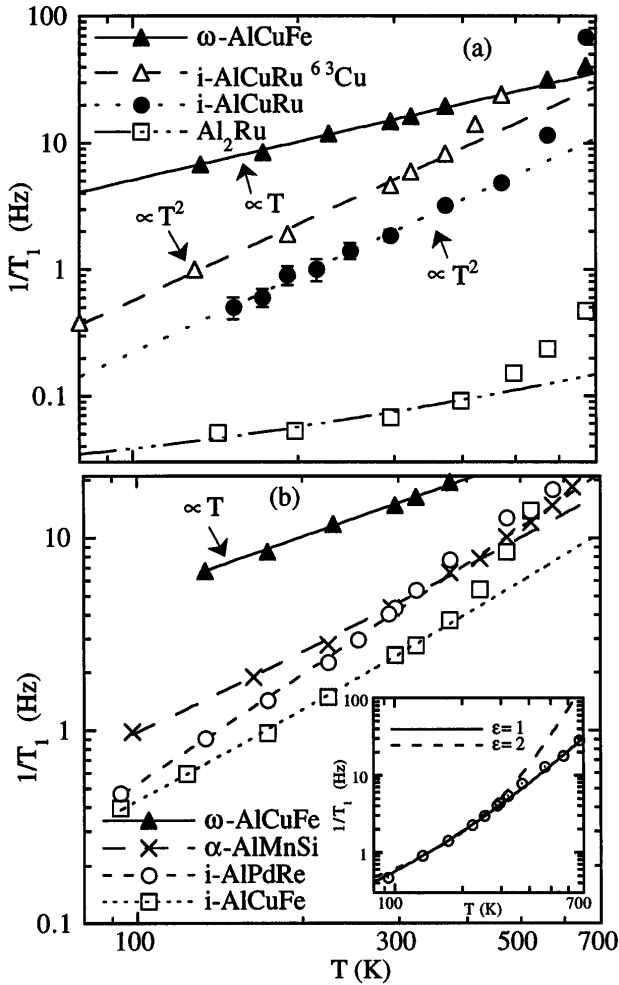


FIG. 2. (a) $1/^{27}\text{T}_1$ versus T in ω -AlCuFe and i -AlCuRu, $10/^{27}\text{T}_1$ versus T in Al_2Ru , and $1/^{63}\text{T}_1$ versus T in i -AlCuRu. The corresponding curves are fits with $1/^{27}\text{T}_1 \propto T$ for ω -AlCuFe and $1/T_1 \propto T^2$ for i -AlCuRu. (b) $1/^{27}\text{T}_1$ versus T in ω -AlCuFe, α -AlMnSi, i -AlPdRe, and i -AlCuFe. The corresponding curves are fits discussed in the text. The inset shows $1/^{27}\text{T}_1$ data in i -AlPdRe fitted with $\varepsilon = 1$ and $\varepsilon = 2$, as discussed in the text. Errors not indicated by error bars are comparable to the sizes of the symbols.

tional form of $M(\tau)$. The $1/^{27}\text{T}_1$ data of i -AlCuRu [Fig. 2(a)] and i -AlPdRe [Fig. 2(b)] (the superscripts 27, 63, and 65 refer to ^{27}Al , ^{63}Cu , and ^{65}Cu , respectively) show a striking feature below 400 K; $1/^{27}\text{T}_1$ is proportional to T^2 rather than to T as observed in ω -AlCuFe. Furthermore, $1/^{63}\text{T}_1$ in i -AlCuRu is also proportional to T^2 below 400 K [Fig. 2(a)]. Significant deviations from $1/^{27}\text{T}_1 \propto T$ are also clearly visible in i -AlCuFe and α -AlMnSi [Fig. 2(b)].

The nature of the relaxation mechanism can be investigated by studying the spin-lattice relaxation of ^{63}Cu and ^{65}Cu in i -AlCuFe and i -AlCuRu. In addition to the contribution via hyperfine couplings, the spin-lattice relaxation of these quadrupolar nuclei could also originate from the quadrupolar interaction [15]. Since ^{63}Cu and ^{65}Cu are spin- $\frac{3}{2}$ nuclei with different quadrupolar moments Q and gyromagnetic ratios γ_n , the two mechanisms can be distinguished by measuring the ratio $^{65}\text{T}_1/^{63}\text{T}_1$. The quadrupolar mechanism leads to $^{65}\text{T}_1/^{63}\text{T}_1 = (Q^{65}/Q^{63})^2 = 1.14$ [15], and the hyperfine interaction leads to $^{65}\text{T}_1/^{63}\text{T}_1 = (\gamma_n^{65}/\gamma_n^{63})^2 = 0.87$ [15]. At room temperature (RT), the measured $^{65}\text{T}_1/^{63}\text{T}_1$ ratio is 0.80–0.87 in i -AlCuFe and 0.83–0.90 in i -AlCuRu, similar to the previous report [14]. Thus, $1/^{63}\text{T}_1$ and $1/^{65}\text{T}_1$ are dominated by hyperfine interactions below RT. Since ^{27}Al possesses very similar Q and γ_n values as the Cu isotopes, the quadrupolar contribution to $1/^{27}\text{T}_1$ is expected to be negligible as well. Furthermore, the quadrupolar contribution associated with phonons can also be estimated from the study of Al_2Ru which has a Debye temperature comparable to all the samples investigated here [2]. Since $1/^{27}\text{T}_1$ in Al_2Ru is at least 100 times smaller than that in all other samples investigated here (Fig. 2), the quadrupolar contribution to $1/^{27}\text{T}_1$ is again expected to be negligible.

In metallic systems, the Fermi contact interaction between conduction s -electron spins and nuclear spins generally dominates the spin-lattice relaxation and the Knight shift [15]. Assuming that the characteristics of the wave function do not change significantly over $k_B T$ around E_F , the Knight shift can be expressed as [15]

$$K_s = \alpha_s \frac{1}{k_B T} \int dE g(E) f(E) [1 - f(E)], \quad (2)$$

where $f(E)$ is the Fermi-Dirac distribution, $g(E)$ is the DOS associated with a single spin orientation, $\alpha_s = (4\pi/3)\hbar^2 \gamma_e^2 \langle |u_k^2(0)| \rangle_{E_F}$, where $\langle |u_k^2(0)| \rangle_{E_F}$ is the density of the wave function at the nucleus averaged over the Fermi surface, and γ_e is the electron gyromagnetic ratio. The spin-lattice relaxation rate is given by [15]

$$(1/T_1)_s = \beta_s \int dE g^2(E) f(E) [1 - f(E)], \quad (3)$$

where $\beta_s = (64/9)\pi^3 \hbar^3 \gamma_e^2 \gamma_n^2 \langle |u_k^2(0)| \rangle_{E_F}^2$. Since $f(E)[1 - f(E)] = -k_B T \partial f(E)/\partial E$ vanishes as E deviates from E_F by a few $k_B T$, the temperature dependences of K_s and $(1/T_1)_s$ are determined by the energy dependence of $g(E)$ near E_F . In typical metals the DOS variation near E_F is

TABLE I. A , B , κ , and K_0 are obtained from fitting $1/^{27}\text{T}$ versus T . The heat capacity constant γ , obtained from Ref. [2], is in units of $\text{mJ} (\text{g atom})^{-1} \text{K}^{-2}$.

	$A ((\text{K s})^{-1/2})$	$B ((\text{K eV s})^{-1/2})$	κ	$K_0 (\text{ppm})$	γ
$i\text{-AlPdRe}$	$<1.0 \times 10^{-2}$	0.57 ± 0.05	0.4 ± 0.1	86 ± 10	0.10
$i\text{-AlCuRu}$	$<1.0 \times 10^{-2}$	0.43 ± 0.03	0.3 ± 0.1	100 ± 10	0.11
$i\text{-AlCuFe}$	$(3.2 \pm 0.9) \times 10^{-2}$	0.32 ± 0.03	-0.2 ± 0.1	86 ± 10	0.31
$\alpha\text{-AlMnSi}$	$(6.5 \pm 0.4) \times 10^{-2}$	0.32 ± 0.05	-0.9 ± 0.1	138 ± 10	0.6
$\omega\text{-AlCuFe}$	$(2.3 \pm 0.1) \times 10^{-1}$...	1.0 ± 0.1	40 ± 10	...

small. Thus, K_s is temperature independent and $(1/T_1)_s \propto T$. The observed significant deviations from $1/T_1 \propto T$ below 400 K indicates that the variation of the DOS near E_F is not small over $k_B T$ around E_F in quasicrystals and approximants.

Assuming that $g(E) = g_0 + g_1|E - E_F|^\varepsilon$, where g_0 is the residual DOS at E_F , Eq. (2) leads to

$$K_s = \alpha_s [g_0 + 2C(\varepsilon)g_1(k_B T)^\varepsilon], \quad (4)$$

where $C(\varepsilon) = \int_0^\infty dx x^\varepsilon e^x / (1 + e^x)^2$, and Eq. (3) leads to

$$(1/T_1)_s = \beta_s k_B T [g_0^2 + 4C(\varepsilon)g_0 g_1 (k_B T)^\varepsilon + 2C(2\varepsilon)g_1^2 (k_B T)^{2\varepsilon}]. \quad (5)$$

For $(k_B T)^\varepsilon (g_1/g_0) \gg 1$, Eqs. (4) and (5) show that $K_s \propto T^\varepsilon$ and $(1/T_1)_s \propto T^{1+2\varepsilon}$, whereas the conventional temperature dependences of K_s and $(1/T_1)_s$ are satisfied for $(k_B T)^\varepsilon (g_1/g_0) \ll 1$. The temperature dependence of $1/T_1$ in $i\text{-AlCuRu}$ and $i\text{-AlPdRe}$ indicates that $\varepsilon \approx \frac{1}{2}$. As shown in Fig. 2, the temperature dependence of $1/T_1$ below 400 K can be fit very well with $1/T_1 = T[A^2 + 4C(0.5)AB(k_B T)^{1/2} + 2C(1)B^2 k_B T]$ ($\varepsilon = \frac{1}{2}$) where the fitting parameters A and B are listed in Table I. Since $(B/A)(k_B T)^{1/2}$ is significantly larger than one in $i\text{-AlCuRu}$, $i\text{-AlPdRe}$, and $i\text{-AlCuFe}$ near RT, the third term (which was neglected previously in a perturbation treatment [12]) is comparable or larger than the second term in Eq. (5). Thus, the previously reported analysis [12] of $1/T_1$ data in $i\text{-AlCuRu}$ with $\varepsilon = 2$ is inaccurate. As an example, the inset of Fig. 2(b) shows that the $1/T_1$ data of $i\text{-AlPdRe}$ cannot be fit with $\varepsilon = 2$ using Eq. (5). Reducing the ε value below one results in reasonable fits as shown in the inset of Fig. 2(b). Overestimation of A values would result from assuming $1/T_1 \propto T$; this could be responsible for the disagreement of some previously reported A values [14] with that shown in Table I. The absence of the third term in Eq. (5) and the assumption of $\varepsilon = 2$ are responsible for the different A value reported previously for $i\text{-AlCuRu}$ [12]. The A values obtained with $\varepsilon = \frac{1}{2}$ are in good agreement with the measured specific heat constant γ which is also proportional to g_0 (Table I). The square-root power law could be found for the DOS at Van Hove-type singularities [6]; it was also predicted by the model of hierarchical packing of atomic clusters in quasicrystals [1].

The Korringa relation [15], $(T_1)_s T K_s^2 = C_s$ with $C_s = (\hbar/4\pi k_B) (\gamma_e^2/\gamma_n^2)$, is also satisfied by Eqs. (4) and (5) for $(k_B T)^\varepsilon (g_1/g_0) \ll 1$. For $(k_B T)^\varepsilon (g_1/g_0) \gg 1$, Eqs. (4)

and (5) give $(T_1)_s T K_s^2 = [2C^2(\varepsilon)/C(2\varepsilon)]C_s$. Thus, $K_s = \sqrt{C_s}/\sqrt{(T_1)_s T}$ should be followed within 10% accuracy over the entire temperature range below 400 K for $\varepsilon = \frac{1}{2}$ and within 25% accuracy for $\varepsilon = 1$. Figure 3 shows the temperature dependence of the shift as well as fits using $K = K_0 + \kappa\sqrt{C_s}/\sqrt{T_1 T}$, where the parameter K_0 accounts for the orbital contribution [15] and the isotropic second-order quadrupolar shift, and the parameter κ characterizes the deviation from the Korringa relation. The good fits with $K = K_0 + \kappa\sqrt{C_s}/\sqrt{T_1 T}$ below 400 K indicate that the novel temperature dependences of the Knight shift and $1/T_1$ are both caused by the sharp feature in the DOS at the Fermi level. Above 500 K, $K = K_0 + \kappa\sqrt{C_s}/\sqrt{T_1 T}$ overestimates the T dependence of the shift because of the contribution of the atomic motion to $1/T_1$ [12]. In $i\text{-AlCuRu}$ and $i\text{-AlPdRe}$ the shifts are positive and increase with increasing T [Fig. 3(a)]; the parameter κ is about $\frac{1}{3}$ (Table I). Such deviation from the Korringa relation can be explained by core polarization contributions to K and $1/T_1$, denoted by K_d and $(1/T_1)_d$, respectively. In

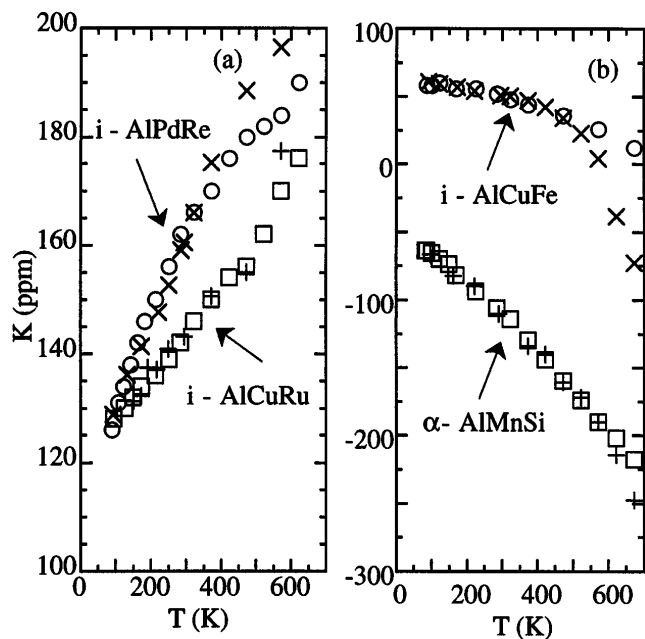


FIG. 3. (a) The measured ^{27}Al shift versus T in $i\text{-AlPdRe}$ (o), $i\text{-AlCuRu}$ (□), and the fits of K based on the measured T_1 data in $i\text{-AlPdRe}$ (x) and $i\text{-AlCuRu}$ (+), as discussed in the text. (b) The measured ^{27}Al shift versus T in $i\text{-AlCuFe}$ (o), $\alpha\text{-AlMnSi}$ (□), and the fits of K based on the measured T_1 data in $i\text{-AlCuFe}$ (x) and $i\text{-AlMnSi}$ (+).

Al alloys with transition elements, the d band at the Fermi level could induce a core polarization hyperfine interaction giving rise to $K = K_0 + K_s + K_d$ with K_d being negative for ^{27}Al . Assuming that the d -band DOS, $g_d(E)$, is given by $g_d(E) = g_{0d} + g_{1d}|E - E_F|^\varepsilon$ near E_F , expressions similar to Eqs. (4) and (5) can be obtained K_d and $(1/T_1)_d$, respectively. The deviation from the Korringa relation in $i\text{-AlCuRu}$ and $i\text{-AlPdRe}$ can be explained by assuming $K_d \approx -0.8K_s$. In $\alpha\text{-AlMnSi}$ [Fig. 3(b)], K decreases as T increases, indicating that $K_s < |K_d|$, which is consistent with the observed negative K values. In $i\text{-AlCuFe}$ [Fig. 3(b)], the small K values and the weak T dependence of K are consistent with nearly equal contributions of K_s and $|K_d|$.

Precise estimation of the width of the DOS valley at E_F is hampered by uncertainties such as the relative contributions of hyperfine interactions caused by conduction s -electron spins and core polarization. Nevertheless, an approximate value can be estimated. Since NMR probes an energy range of about $k_B T$ around E_F , a measure of ΔE , where $g(E_F \pm \Delta E/2) \approx 2g_0$, is $k_B T^*$ and T^* is the temperature above which $1/T_1$ exhibits significant deviations from $1/T_1 \propto T$. In $i\text{-AlCuFe}$, T^* is about 150 K which leads to $k_B T^* = 13$ meV. This estimate agrees with the estimation of ΔE based on the A and B values listed in Table I. Since the ratio B/A in $i\text{-AlCuFe}$ is $10 \text{ eV}^{-1/2}$, $g(E) = g_0 + g_1|E - E_F|^{1/2}$ increases to $2g_0$ at $E = E_F \pm 10$ meV. In $i\text{-AlCuFe}$, the specific heat measurement shows that g_0 is about one-third of the estimated free-electron value, which serves as an upper limit of DOS at E_F without the DOS valley [2,3]. Thus, $\Delta E \approx 20$ meV can serve as an estimated width of the sharp DOS feature in $i\text{-AlCuFe}$. In $i\text{-AlPdRe}$ and $i\text{-AlCuRu}$, specific heat measurements show that g_0 is about one-tenth of the estimated free-electron value [2]. The estimated widths of the DOS valley in $i\text{-AlPdRe}$ and $i\text{-AlCuRu}$ are of the same order of magnitude as in $i\text{-AlCuFe}$ based on the B/A ratio of about $50 \text{ eV}^{-1/2}$ (Table I). Tunneling experiments reveal a similar width of about 50 meV for the sharp feature in the DOS at the Fermi level [8]; however, the form of the narrow gap obtained here is $g(E) = g_0 + g_1|E - E_F|^\varepsilon$ with $\varepsilon \approx 1.8\text{--}2$ rather than $\frac{1}{2} \leq \varepsilon \leq 1$. Given the uncertainties in both the NMR and the tunneling experiments, such a discrepancy could not be clarified based on the currently available information.

In conclusion, the novel temperature dependences of $1/T_1$ and the Knight shift in quasicrystalline alloys reveal the presence of a sharp DOS valley around E_F ; the width of this sharp feature is on the order of 20 meV. This sharp feature is much narrower than the broad pseudogap

of about 0.5–1.0 eV. The observed sharp DOS valley could have significant influence on the transport properties of quasicrystals.

This work was supported by the National Science Foundation under Contracts No. DMR-9520477 and No. DMR-9319084.

-
- [1] C. Janot, *Quasicrystals: A Primer* (Clarendon, Oxford, 1994).
 - [2] B.D. Biggs, S.J. Poon, and N.R. Munirathnam, Phys. Rev. Lett. **65**, 2700 (1990); B.D. Biggs, Y. Li, and S.J. Poon, Phys. Rev. B **43**, 8747 (1991); S.J. Poon, Adv. Phys. **41**, 303 (1992); F.S. Pierce, S.J. Poon, and B.D. Biggs, Phys. Rev. Lett. **70**, 3919 (1993); F.S. Pierce, Q. Guo, and S.J. Poon, Phys. Rev. Lett. **73**, 2220 (1994).
 - [3] T. Klein, C. Berger, D. Mayou, and F. Cyrot-Lackmann, Phys. Rev. Lett. **66**, 2907 (1991).
 - [4] H. Matsubara, S. Ogawa, T. Kinoshita, K. Kishi, S. Takeuchi, K. Kimura, and S. Suga, Jpn. J. Appl. Phys. **30**, L389 (1991); E. Belin, Z. Dankhazi, A. Sadoc, Y. Calvayrac, T. Klein, and J.M. Dubois, J. Phys. Condens. Matter **4**, 4459 (1992).
 - [5] M. Mori, S. Matsuo, T. Ishimasa, T. Matsuura, K. Kamiya, H. Inokuchi, and T. Matsukawa, J. Phys. Condens. Matter **3**, 767 (1991).
 - [6] X. Wu, S.W. Kycia, C.G. Olson, P.J. Benning, A.I. Goldman, and D.W. Lynch, Phys. Rev. Lett. **75**, 4540 (1995).
 - [7] Z.M. Stadnik, D. Purdie, M. Garnier, Y. Baer, A.-P. Tsai, A. Inoue, K. Edagawa, and S. Takeuchi, Phys. Rev. Lett. **77**, 1777 (1996).
 - [8] T. Klein, O.G. Symko, D.N. Davydov, and A.G.M. Jansen, Phys. Rev. Lett. **74**, 3656 (1995); D.N. Davydov, D. Mayou, C. Berger, C. Gignoux, A. Neumann, A.G.M. Jansen, and P. Wyder, Phys. Rev. Lett. **77**, 3173 (1996).
 - [9] T. Fujiwara, J. Non-Cryst. Solids **156–158**, 865 (1993); G.T. de Laissardiere and T. Fujiwara, Phys. Rev. B **50**, 5999 (1994); M. Krajci, M. Windisch, J. Hafner, G. Kresse, and M. Mihalkovic, Phys. Rev. B **51**, 17355 (1995).
 - [10] Ph. Ebert, M. Feuerbacher, N. Tamura, M. Wollgarten, and K. Urban, Phys. Rev. Lett. **77**, 3827 (1996).
 - [11] S. Matsuo, H. Nakano, T. Ishimasa, and Y. Fukano, J. Phys. Condens. Matter **1**, 6893 (1989).
 - [12] E.A. Hill, T.C. Chang, Y. Wu, S.J. Poon, F.S. Pierce, and Z.M. Stadnik, Phys. Rev. B **49**, 8615 (1994).
 - [13] F. Hippert, L. Kandel, Y. Calvayrac, and B. Dubost, Phys. Rev. Lett. **69**, 2086 (1992).
 - [14] A. Shastri, F. Borsa, D.R. Torgeson, J.E. Shield, and A.I. Goldman, Phys. Rev. B **50**, 15651 (1994).
 - [15] J. Winter, *Magnetic Resonance in Metals* (Clarendon, Oxford, 1971).